SOME ASPECTS OF THE ULTRASTRUCTURE AND ENZYME CYTOCHEMISTRY OF NORMAL AND VIRUS-TRANSFORMED CELLS

by

ALAN LESLIE DAWSON

of the

School of Biological Sciences, Thames Polytechnic, London.

A thesis presented for the degree of Doctor of Philosophy to the Council for National Academic Awards.

August, 1976.

VOLUME II

INDEX TO PLATES

FIGS. 87 & 88. BHK21C13 cells centrifuged to a pellet prior to incubation.

89 - 92. Normal and transformed 3T3 cells incubated <u>in situ</u> followed by centrifugation to a pellet.

89 - 91. 3T3.

92. SV403T3.

93 - 99. The LPED procedure for acid phosphatase demonstration.

93. BHK21C13.

94 - 97. Mouse kidney cortex.

98 & 99. Mealworm midgut epithelium.

100. Formol-calcium fixation of BHK21C13.

101 - 104. The lead phthalocyanin procedure for acid phosphatase demonstration, applied to mouse kidney cortex.

105 & 106. Mouse kidney cortex incubated in the presence of precursors of LPED.

105. Hexaphenyl lead.

106. Triphenyl-p-amino-phenethyl lead.

107 & 108. The p-nitrobenzene-diazonium tetrafluoroborate (NDFB) procedure for acid phosphatase demonstration, applied to mouse kidney cortex.

109 - 113. The hexazonium pararosaniline (HPR) procedure for acid phosphatase demonstration, applied to mouse kidney cortex.

114. Mouse kidney cortex, not subjected to cytochemical tests.

115. BHK21J1. Esterase demonstration by the thiolacetic acid method.

116 - 127. Arylsulphatase demonstration by the barium-nitrocatechol sulphate method.

116 - 118. Chick embryo fibroblasts (CEF).

119 - 122. ts virus-infected CEF maintained at 35^{o}C.

123 - 126. ts virus-infected CEF maintained at 41^{o}C.

127. SV403T3.

FIG. 1

BHK21C13. These typical fibroblasts are elongated and grow in close-packed parallel orientation with little overlapping. Individual cells are mainly spindle-shaped with two major cell processes. X 900

FIG. 2

BHK21J1. These transformed cells, unlike the normal C13 cells, are randomly orientated and tend to pile up and overlap each other. They have two or more major cell processes, often with long, fine extensions. Some cells are rounded up for division. X 900

FIG. 3

3T3. Confluent 3T3 cells are epithelioid. They are extremely thin and flat with little or no overlapping. Nuclei are large with prominent nucleoli. X 750

FIG. 4

SV40 3T3. Most cells are fibroblastic although some large flattened ones do occur. Cells usually have more than two major cell processes, the cytoplasm is granular and often vacuolated. There is much overlapping and piling up of cells. X 750

FIG. 5

Chick embryo fibroblasts (CEF). At both 35°C and 41°C these cells are fibroblastic with two or more major cell processes and cytoplasm that is often vacuolated. The cells usually grow randomly and overlap but occasionally exhibit parallel orientation. X 750

FIG. 6

ts virus-infected CEF at 35°C. At this, the permissive temperature for action of the viral genes for transformation, the cells are transformed. Two types of cell are present, small dense fibroblasts and the more numerous small rounded cells which are dense and refractile. X 750

FIG. 7

ts virus-infected CEF at 41°C. At this non-permissive temperature infected cells are not transformed and are indistinguishable from uninfected cells (compare Fig. 5) X 750

FIG. 8

General field of BHK21C13 cells prepared by centrifugation to a pellet. Some cells and nuclei are misshapen and distorted, there are numerous large spaces in the cytoplasm and there is much extracellular debris which appears to be derived from disrupted cells. Cell surfaces are mainly smooth. Mitochondria are small and dense (arrows). X 7,500

FIG. 9

Centrifuged BHK21C13 cell with an irregular nucleus. At the cell surface are a number of microvilli, two of which appear to be combining to form a pinocytic vesicle (arrow). Other pinocytic vesicles (pv) are present in the cytoplasm. Fuzzy material on the surface may represent a cell coat (double arrow). Mitochondria (m) are small and dense and secondary lysosomes (sl) can be identified.

X 13,000

FIG. 10

The nuclear membrane of this BHK21C13 cell is irregular (arrows). A secondary lysosome (sl) is present and just below the surface can be seen micropinocytic vesicles. Possible cell coat material is on the cell surface (double arrow) and two possible cell junctions (cj) can be seen. X 33,750.

FIG. 11

Nuclear pores (np) can be detected in the nuclear membrane of this BHK21C13 cell. In the cytoplasm are distended rough ER cisternae (arrow) and secondary lysosomes (sl). Masses of microfilaments (mf) are in close proximity to the Golgi region (g) in which the elements are somewhat swollen and irregular. A centriole (c) is also present.

X 13,000

FIG. 12

This BHK21C13 cell has a very irregular nucleus. The nuclear membrane is also irregular and has nuclear pores (np). A secondary lysosome (sl) in the cytoplasm exhibits traces of double membrane. Some elements of the Golgi complex (G) appear swollen and several microtubules (mt) can just be distinguished between nucleus and Golgi.

X 21,000

FIG. 13

Golgi region of BHK21C13 cell. Microfilaments (mf) are present throughout the region and Golgi vesicles (Gv), which are probably synonymous with primary lysosomes, are clustered around the larger Golgi components. There is a possible example of the sequestration of a portion of cytoplasm by membrane formation (arrows) around the area in question. X 50,000

FIG. 14

In the cytoplasm of this BHK21C13 cell is an autolysosome (al) which contains a mitochondrion, cytoplasmic ground substance, ribosomes and membranous material. None of these components appear to have undergone much breakdown and this fact, coupled with the presence of sections of double membrane around the lysosome (arrow), indicates that autolytic activity is only just commencing. Cisternae of the rough ER (rer) are markedly distended. X 52,000

FIG. 15

General field of <u>in situ</u> embedded BHK21C13 cells (compare with Fig. 8). The largely smooth-surfaced cells lie in close-packed, parallel orientation. Nuclei are mainly ovoid and in the cytoplasm are many organelles and some clear spaces. X 6,000

FIG. 16

Enlargement of part of Fig. 15. The cytoplasmic spaces (cs) are clearly not membrane bound and amongst the organelles can be distinguished at least one pinocytic vesicle (pv). Along part of the plasma membrane (long arrow) a number of smooth micropinocytic vesicles are being formed. There is a possible connection between nuclear envelope and rough ER (short arrow). X 10,000

FIG. 17

Golgi region of BHK21C13 cell. Dense masses of microfilaments (mf) are found throughout this poorly developed Golgi complex. Small dense Golgi vesicles (Gv) are common and a pair of centrioles (c) is present. Close to several secondary lysosomes is a multivesicular body (mvb). Amorphous extracellular material (arrow) may represent part of a cell coat. X 20,000

FIG. 18

Three types of skeletal element are present in the cytoplasm of these adjacent BHK21C13 cells. Microfilaments (mf) occur throughout the cytoplasm and in bundles beneath the cell surface. Filaments (f) are orientated along the centre of the cell process, as also are some of the microtubules (mt). At the cell surface micropinocytosis is in evidence through the formation of coated (arrow) or smooth (double arrow) micropinocytic vesicles. Possible cell junctions (cj) are made between the two cells. Sections of rough ER (rer) are present and some are closely aligned to a large ovoid mitochondrion (m). X 20,000

FIG. 19

BHK21C13. A cell junction (cj) is made between two cells and in the cytoplasm of one of them rough ER (rer) is in close association with mitochondria. X 30,000

FIG. 20

BHK21C13. There is a bridge-like connection (b), formed by two entwined microvilli, between two cells. Randomly orientated microfilaments (mf) are abundant around the periphery of the Golgi complex (G) and a multivesicular body (mvb) is also present. Small dense Golgi vesicles are found throughout this area. X 42,000

FIG. 21

SHK21C13. There is evidence of cell coat material (arrow) between two closely aligned sections of plasma membrane. Also at the cell surface can be seen the formation of a coated micropinocytic vesicle (cmv). Filaments (f) and microtubules (mt) are present in the cytoplasm and numerous Golgi vesicles (Gv) are clustered around a secondary lysosome and other vacuoles. X 40,000

FIG. 22

BHK21C13. A pair of centrioles (c) is present in the Golgi region (G) and one of these centrioles serves as the basal body of a cilium (ci) which penetrates the cytoplasm of a neighbouring cell. An autolysosome (al) exhibiting traces of double membrane is near to clusters of Golgi vesicles. A nuclear pore (arrow) can be seen in the nuclear envelope. X 40,500

FIG. 23

The nuclei of these BHK21J1 cells have dense, granular nucleoli. Some of the mitochondria in the cytoplasm are intimately surrounded by sections of rough ER (arrow). X 18,750

FIG. 24

These two BHK21J1 cells have irregular nuclei. In the cytoplasm there are extensive Golgi complexes (G) and mitochondria are closely associated with short sections of rough ER. X 10,000

FIG. 25

BHK21J1. The microvilli (mvi) at the leading edge of the upper cell appear to be probing the environment immediately before them. In the cytoplasm of the lower cell are masses of small vesicles (v), probably of Golgi origin. X 17,500

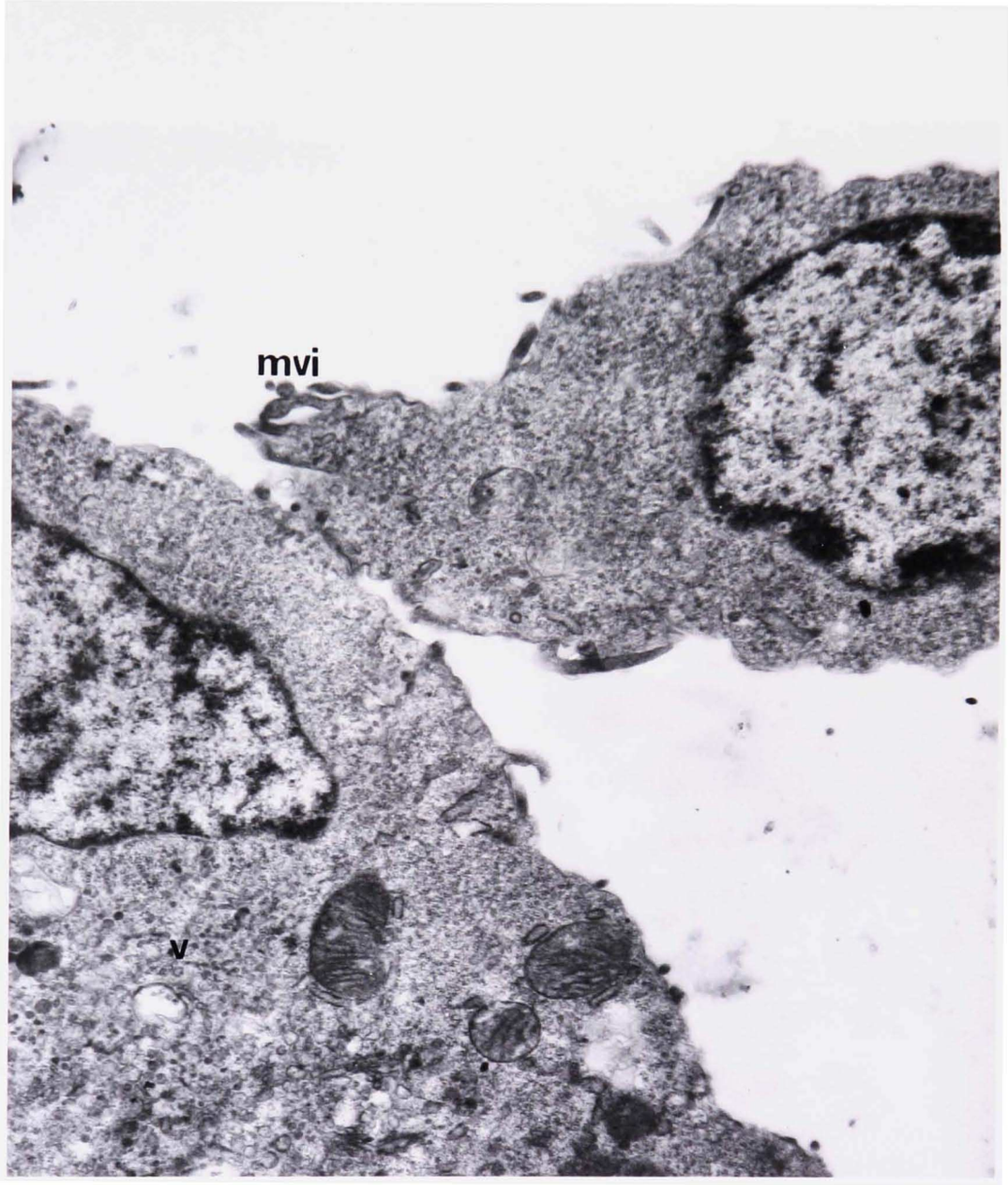
mvi
v

FIG. 26

BHK21J1. Microvilli (arrow) are present at the cell surface whilst prominent in the cytoplasm are a number of autolysosomes (al) and residual bodies (rb). The former contain material of cytoplasmic origin, mainly cytoplasmic ground substance, ribosomes and mitochondria. Residual bodies may fuse together and contain dense material and membranous fragments. In the nucleus is an intranuclear body (inb) of uncertain function. X 20,000

FIG. 27

BHK21J1. These two cells, one of which has an irregular nucleus, appear to make contact by complexes of microvilli (arrows). In the Golgi region (G) are masses of microfilaments and numerous small vesicles. Multivesicular bodies (mvb) are also present. Sections of rough ER, some of which are branched and slightly expanded, are in close association with mitochondria. One such mitochondrion (m) appears to be undergoing breakdown. X 14,000

FIG. 28

BHK21J1. This cell has an extremely irregular nucleus which contains an intranuclear body (inb) of uncertain function. Residual bodies (rb), containing myelin figures, are prominent in the cytoplasm and one of them appears to be exocytosed (arrow). X 20,000

FIG. 29

BHK21J1. In the lower of these two cells a coated micropinocytic vesicle (cmv) is being formed whilst in the upper cell a similar vesicle is fusing with a larger body (arrow). Throughout the Golgi region (G) are masses of microfilaments. Opaque bodies (o) which are not membrane bound are present in the lower cell. X 30,000

FIG. 30

BHK21J1. This cell has rounded up for mitosis and exhibits chromosomes arranged in a circular configuration. There are a number of microvilli at the cell surface. X 15,750

FIG. 31

BHK21J1. Amorphous material on the cell surface (short arrow) may represent evidence of a cell coat. There is also a possible example of phagocytosis (ph) at the cell surface. In the cytoplasm is a large multivesicular body (mvb) and an autolysosome (al) exhibiting a section of double membrane, (long arrow) suggesting that autolysis is only just commencing. X 38,000

FIG. 32

BHK21J1. A coated micropinocytic vesicle (cmv) is being formed at the plasma membrane. There is a cytoplasmic space (cs) which is not membrane bound and contains condensed masses of cytoplasm. Adjacent to it is a small opaque region and a band of microfilaments. X 30,000

FIG. 33

BHK21J1. Dense bands of parallel orientated filaments (f) are found immediately beneath the plasma membrane of this cell process. The prominent feature is the profusely branched and expanded rough ER (rer) which contains a flocculent, opaque material. This ER is very closely associated with mitochondria, two of which (m) appear to be undergoing breakdown. A cytoplasmic space (cs), surrounded by filaments, contains a few membranous fragments. X 30,000

FIG. 34

BHK21J1. Almost half the width of this cell process is occupied by a dense band of parallel orientated filaments (f) adjacent to the plasma membrane. A cytoplasmic space (cs) is associated with membranous material and a large autolysosome (al), containing a variety of cytoplasmic matter, exhibits a section of double membrane (arrow), indicating that autolysis has probably only recently commenced. X 40,000

FIG. 35

BHK21J1. This is the central area of the circle of chromosomes shown in Fig. 30. A single centriole (c) is present and there is a profusion of microtubules (mt), seen largely in transverse and tangential section. These microtubules are presumably acting as spindle fibres.

X 40,000

FIG. 36

BHK21J1. In this Golgi region is a pair of centrioles (c). The two centrioles lie at right angles to each other and are surrounded by Golgi vesicles and microfilaments. X 43,000

FIG. 37

General field of 3T3 cells. The epithelioid nature of these cells is apparent. Microvilli (mvi) may make contacts between cells whilst some microvilli and surface folds (arrows) appear to be involved in pinocytosis. The large, fairly regular nuclei have several nucleoli, some of which exhibit pronounced pars amorpha (pa) and pars granulosa (pg). The cytoplasm is packed with organelles. Lipid droplets (ld) occur frequently, often in clusters, whilst the most prominent organelles are the residual bodies, some of which are large (rb) and others small. The small residual bodies are much more abundant and at this low magnification are difficult to distinguish from mitochondria. Cytoplasmic spaces (cs) are present and sometimes have organelles intruding into them. X 6,000

FIG. 38

3T3. The presence of amorphous material on the cell surface (long arrow) may be indicative of a cell coat. There is a possible cell junction (cj) and beneath the plasma membrane in this region are bundles of filaments. A coated micropinocytic vesicle (cmv) is present near the cell surface and there are two lipid droplets (ld) which have dark outer rims. An autolysosome (al) contains cytoplasmic ground substance and ribosomes. The small, dense residual bodies (rb) are distinguishable from mitochondria and often contain membranous fragments. Where rough ER is in close association with mitochondria it is sometimes devoid of ribosomes on its surface (short arrow). There is a small cytoplasmic inclusion (ci) into the nucleus. X 16,000

FIG. 39

3T3. Micropinocytosis by formation of smooth micropinocytic vesicles is observed at the cell surface (arrows), below which a band of filaments (f) occurs. There is an extensive Golgi complex (G) and a secondary lysosome with a light granular, homogeneous content (hsl) is also present. X 10,500

FIG. 40

3T3. The formation of a coated micropinocytic vesicle (cmv) is taking place at the plasma membrane whilst close to the cell surface are masses of microfilaments (mf) and a number of filaments (f), some of which are serpentine. In the cytoplasm, where residual bodies are prominent, are autolysosomes (al) containing cytoplasmic ground substance. X 31,500

FIG. 41

3T3. The elements of the Golgi complex (G) of this cell are well defined. There are flattened saccules, more irregular, distended vacuoles and small dense vesicles. In addition to sections of rough ER there are also elements of a system of smooth ER (ser) which present a much more varied and irregular appearance than the rough ER. In at least one place (short arrow) the two systems are seen to be connected. Where rough ER and a mitochondrion are closely associated the ER is devoid of its surface ribosomes (long arrow). A homogeneous secondary lysosome (hsl) is also present. X 40,000

FIG. 42

3T3. Part of a very extensive Golgi complex is illustrated. Golgi saccules and vacuoles are outnumbered by smooth ER (ser) elements which vary from small rounded vesicles to extended branching profiles. Their matrix is denser than that of rough ER. A sac-like body (slb) is in continuity with the smooth ER and there is a large flattened saccule (fs) which may be either a Golgi or smooth ER component. Small dense vesicles are produced by this saccule and "budded-off" its convoluted surface. Such vesicles, derived from smooth ER and Golgi apparatus, are believed to represent primary lysosomes and some of them are apparently fusing with larger vacuoles (v) into which they release their contents (short arrows). The vesicles are present throughout the region as also are microtubules (mt). A regularly striated structure (long arrow) probably represents a connective tissue fibre. A centriole (c) and a signet-ring lysosome (sr) also occur in this area. X 30,000

FIG. 43

3T3. Adjacent to the nucleus, which has well-defined nuclear pores (np) in its envelope, is an extensive Golgi complex in which stacks of up to seven flattened saccules are prominent. Smooth ER is also present and is seen to be in continuity with rough ER (arrows). Small dense vesicles, presumably primary lysosomes, are found throughout the region and some of them appear to fuse with larger vacuoles (v). Microtubules and filaments are also frequent and a multivesicular body (mvb) and a signet-ring lysosome (sr) are present. X 30,000

FIG. 44

3T3. In this Golgi region it is difficult to distinguish between Golgi and smooth ER elements. To one side of the complex is a body which appears to represent a late stage in the sequestration of a portion of cytoplasm, i.e. a cytosegresome (cs). This sequestration is probably performed by Golgi or smooth ER membranes. The contents of the body are not broken down and the double membrane is virtually complete so that it is unlikely that any autolysis has taken place.

X 40,000

FIG. 45

General field of SV403T3 cells. The cell surfaces have numerous small folds and convolutions and the coalescence of such folds is probably responsible for pinocytosis (arrow). Cell junctions are observed (double arrow). The most obvious difference from 3T3 cells is the absence from the cytoplasm of the numerous small, dense residual bodies (compare with Fig. 37). One cell has a very large circular vacuole (v) which contains membranous fragments. X 6,000

FIG. 46

General field of SV403T3 cells. Cell and nuclear shape are variable and the cell surface is much folded and convoluted except where cells are very close-packed. Cytoplasmic organelles are not as prominent as those of 3T3 cells (compare Fig. 37). X 6,300

FIG. 47

SV403T3. Extracellular material (arrows) is mainly of a fibrous nature but some of it could represent part of a cell coat. A cell junction (cj) is present. The ring-shaped nucleus presumably appears thus as a result of having a large indentation of its upper or lower surface. Three types of secondary lysosome are found in the cytoplasm. An autolysosome (al) contains cytoplasmic ground substance whilst a large dense body lysosome (db) has a largely homogeneous content. A multivesicular body (mvb) is also present. X 10,000

FIG. 48

SV40 3T3. This is an enlargement of part of Fig. 47. A smooth micropinocytic vesicle (smv) is forming at the plasma membrane and it may be destined to fuse with the secondary lysosome in the cytoplasm immediately beneath it. One cell has a fairly extensive Golgi complex (G), though not on the same scale as those of 3T3 cells. The nuclear envelope is noticeably uneven whilst in the nucleus two of the nucleoli have pronounced pars amorpha (pa) and pars granulosa (pg). In the area of cytoplasm enclosed by the nucleus one mitochondrion contains a dense body (arrow) and another has amongst its cristae one that is circular (cr). Where the rough ER is in close proximity to mitochondria it is devoid of its surface ribosomes (double arrow). Dense body secondary lysosomes (db) are also present. X 20,000

FIG. 49

SV40 3T3. Intercellular contact between two of these cells appears to be made by microvilli (arrow). Coated micropinocytic vesicles (cmv) are found in the cytoplasm near the cell surface and microtubules are orientated roughly parallel along the cell processes (double arrow). Small dense primary lysosomes (pl) are seen and a signet-ring lysosome (sr) is also present. X 30,000

FIG. 50

SV403T3. In this Golgi region elements of the Golgi complex and smooth ER are sometimes difficult to distinguish from each other. Small dense vesicles are abundant and clusters of lipid droplets (ld) occur. Microtubules are present (arrow) and a centriole acts as the basal body of a cilium (ci). X 30,000

FIG. 51

SV403T3. The prominent feature is the large residual body (rb) containing dense membranous and amorphous material. Other components of the lysosomal system present are a small multivesicular body (mvb), a signet-ring lysosome (sr) and primary lysosomes or Golgi vesicles (Gv). Filaments are found in the cytoplasm and one (f) runs parallel with a microtubule (mt). The rough ER is in continuity with the nuclear envelope (long arrow). A coated micropinocytic vesicle (cmv) lies just beneath the cell surface whilst a smooth micropinocytic vesicle (smv) is being formed at the plasma membrane. Indistinct material on the cell surface may represent part of a cell coat (short arrows). X 31,500

FIG. 52

General field of chick embryo fibroblasts. Two of these irregularly shaped cells appear to make a bridge-like connection (b) by means of microvilli. The cytoplasm is packed with organelles, predominantly components of the lysosomal system. Many of these lysosomes are very large, probably as a result of fusion of two or more individuals. Autolysosomes (al) contain cytoplasmic material in varying stages of breakdown whilst other secondary lysosomes (sl) appear to initially have a fine, granular, homogeneous matrix which, owing to degradation of contents or fusion with other bodies, accumulates myelin figures and denser material. Lipid droplets (ld) are also numerous and appear to enlarge by fusion. X 6,000

FIG. 53

General field of chick embryo fibroblasts. These cells have a more regular appearance than those of Fig. 52. Nuclei are also quite regular and the nucleoli can be seen to have thread-like nucleonemata (no). At the cell surface pinocytosis (p) is achieved by coalescence of surface folds or microvilli whilst micropinocytosis is rare, few vesicles being observed (small arrow). A cell junction is present (large arrow). In the cytoplasm many of the mitochondria are elongated and often serpentine or branched (m). Most of them exhibit dense bodies in the matrix, a common feature when Durcupan dehydration is utilised. Secondary lysosomes (sl) with a largely homogeneous content are common as also are autolysosomes (al). X 6,000

FIG. 54

General field of chick embryo fibroblasts. A bridge-like connection (b) of microvilli is made between two of these cells whilst a specialised cell junction is also seen (broad arrow). There is a certain amount of extracellular material (ex), largely of a membranous nature, and the presence of myelin figures outside the cell indicates that a process of exocytosis or defaecation (de) of residual body contents has occurred. Bands of filaments are found just beneath the cell surface (arrows) and cisternae of the rough ER (rer) are extended, branched and frequently expanded with an opaque matrix. Secondary lysosomes (sl) with a homogeneous content are present and residual bodies (rb) containing dense myelin figures also occur. X 6,000

FIG. 55

Chick embryo fibroblast. In this Golgi region the elements of the Golgi complex are not well differentiated and are difficult to distinguish from smooth ER components. Small dense Golgi vesicles are abundant and several Golgi vacuoles (Gva) also occur. Filaments and microfilaments are found throughout the region and a pair of centrioles (c) is present. Autolysosomes (al) contain partially degraded mitochondria, cytoplasmic ground substance and ribosomes. A number of bodies are probably early autolysosomes or autophagosomes (ap) since they appear like lysosomes surrounded by a double membrane. The formation of such bodies seems to be achieved by the enclosure of portions of cytoplasm by smooth ER or Golgi cisternae (arrows). One of the autophagosomes is connected to a short length of a structure (broad arrow) which is presumably derived from a Golgi or smooth ER component. X 21,000

FIG. 56

ts virus-infected chick embryo fibroblasts at 35°C. In these transformed cells there are more cell junctions (arrows) than in the normal cells. The cytoplasm has fewer mitochondria and a great reduction in the number of lysosomes. The rough ER exhibits no expansion of its cisternae. X 10,500

FIG. 57

ts virus-infected chick embryo fibroblasts at 35°C. These transformed cells have far more microvilli and surface extensions than normal cells. The cytoplasm contains fewer organelles, particularly lysosomes.

X 6,000

FIG. 58

BHK21C13. Acid phosphatase demonstration by the Gomori lead-salt method. Acid phosphatase activity, as demonstrated by the dark brown deposits of lead sulphide end product, is localised in particulate fashion throughout the cytoplasm but particularly in the perinuclear region where there are often clusters of dense particles. The cells exhibit characteristic close-packed parallel orientation. X 950

FIG. 59

BHK21J1. Acid phosphatase demonstration by the Gomori lead salt method. As in the normal cells the dark brown deposits of lead sulphide end product are distributed throughout the cytoplasm in a particulate fashion, with most particles in the perinuclear region. The cells are randomly orientated and some are in mitosis. X 950

FIG. 60

3T3. Acid phosphatase demonstration by the naphthol AS-BI phosphate - Fast Red Violet LB salt method. Acid phosphatase activity is indicated by the deposition of red azo-dye. Deposits of this azo-dye are distributed throughout the cytoplasm in a fine, particulate manner, with some concentration around the nucleus. The particles are much more abundant than the Gomori end product deposits in the BHK cells and presumably reflect the extensive lysosome system seen in the morphological study. The epithelioid cells are extremely flat and form a confluent monolayer. X 1,250

FIG. 61

SV403T3. Acid phosphatase demonstration by the naphthol AS-BI phosphate - Fast Red Violet LB salt method. In these fibroblastic transformed cells there do not appear to be as many particles of azo-dye end product as in the 3T3 cells but particles are often larger and much more intensely coloured. This is particularly noticeable in the perinuclear region. In both the normal and transformed 3T3 cells the other enzymes demonstrated by azo-dye techniques have similar localisations to acid phosphatase although there are differences in levels of activity. X 1, 250

FIG. 62

Chick embryo fibroblasts (CEF). Acid phosphatase demonstration by the naphthol AS-BI phosphate - Fast Red Violet LB salt method. The acid phosphatase results in all the chick cells are similar to those obtained for the other enzymes demonstrated by azo-dye methods. In these uninfected normal cells the red azo-dye end product has a particulate distribution throughout the cytoplasm. Particle size is variable, some being comparatively large and irregular. X 1,250

FIG. 63

ts virus-infected CEF, maintained at 35°C. Acid phosphatase demonstration by the naphthol AS-BI phosphate - Fast Red Violet LB salt method. Many of these distinctive small, dense transformed cells exhibit very little or no end product deposition. However, those cells which do display enzyme activity contain large, intensely coloured azo-dye deposits. There does not appear to be any morphological difference between these two classes of cell. X 1,250

FIG. 64

ts virus-infected CEF, maintained at 41°C. Acid phosphatase demonstration by the naphthol AS-BI phosphate - Fast Red Violet LB salt method. These cells have the same morphological appearance as the normal, uninfected CEF cells and, like the latter, all exhibit some degree of red azo-dye deposition of a particulate nature. Some of the cells are rounded, possibly for division, and these exhibit large, irregular, intensely coloured deposits similar to those observed in the infected cells maintained at 35°C. X 1,250

FIG. 65

BHK21C13. Acid phosphatase demonstration by the Gomori method. Dense deposits of lead phosphate end product, indicating acid phosphatase activity, are localised in saccules and vesicles of the Golgi complex (arrows) and in secondary lysosomes (sl). These secondary lysosomes have small dense areas in an otherwise homogeneous matrix and it is only in these denser areas that end product is not deposited.

X 30,000

FIG. 66

BHK21C13. Acid phosphatase demonstration by the Gomori method. Of this group of autolysosomes about half of them exhibit deposits of lead phosphate end product of acid phosphatase activity (arrows). The deposits are associated with the cytoplasmic content of the autolysosomes. X 25,000

FIG. 67

BHK21C13. Acid phosphatase demonstration by the Gomori method. Dense deposits of lead phosphate end product are localised in an autolysosome (arrow). Sparser deposits occur in another autolysosome whilst much of the cytoplasm exhibits a certain amount of "background" lead deposition which parallel no-substrate control incubations prove to be unrelated to acid phosphatase activity. X 25,000

FIG. 68

BHK21C13. Acid phosphatase demonstration by the Gomori method. Three autolysosomes (al) exhibit sparse lead phosphate end product deposits whilst in the cytoplasm immediately surrounding them there is considerable deposition. Since control incubations do not demonstrate background lead deposition in a similar situation it seems likely that in this cell there is acid phosphatase activity in the cytoplasm around the autolysosomes, probably resulting from enzyme leakage. X 30,000

FIG. 69

BHK21J1. Acid phosphatase demonstration by the Gomori method. There are very dense deposits of lead phosphate end product in two secondary lysosomes (arrows). Any fine-structural details within the lysosomes is masked by the end product. Background lead deposition, unrelated to enzyme activity, occurs quite uniformly throughout the nucleus (N) and cytoplasm, including mitochondria (m). Only the lipid droplets (ld) are free of lead. X 39,000

FIG. 70

BHK21J1. Acid phosphatase demonstration by the Gomori method. Lead phosphate end product is confined between the two membranes surrounding an autolysosome (arrow). The presence of acid phosphatase activity at this site could indicate that the autolysosome has been formed by the sequestration of an area of cytoplasm by Golgi or smooth ER components containing the enzyme. X 52,000

FIG. 71

BHK21J1. Acid phosphatase demonstration by the Gomori method. Lead phosphate end product deposition indicates that acid phosphatase activity is localised within saccules and vesicles of the Golgi complex (small arrows) and in a lysosome, the structure of which is hidden by the dense end product (large arrow). X 52,000

FIG. 72

3T3. Acid phosphatase demonstration by the Gomori method. The lead phosphate end product of acid phosphatase activity is confined to secondary lysosomes (sl), probably autolysosomes, and is associated with membranous and other contents. X 37,500

FIG. 73

3T3. Acid phosphatase demonstration by the Gomori method. Deposition of lead phosphate end product in the secondary lysosomes (sl) is so heavy that underlying detail is hidden. In the irregular residual body (rb), however, deposition is much lighter and represents enzyme activity remaining on completion of degradative activity. X 30,000

FIG. 74

3T3. Acid phosphatase demonstration by the Gomori method. Lead phosphate end product deposits are localised in saccules and vesicles of the Golgi complex (arrows). Background lead deposition, unrelated to enzyme activity, occurs in the nucleus (N). X 50,000

FIG. 75

SV403T3. Acid phosphatase demonstration by the Gomori method. A secondary lysosome (sl) is the site of lead phosphate end product deposition which shows the enzyme to have a patchy distribution within a fairly homogeneous matrix. X 50,000

FIG. 76

SV403T3. Acid phosphatase demonstration by the Gomori method. Lead phosphate end product is associated with the membranous and amorphous material in a large residual body (rb). In addition there is a regular deposition throughout a cell coat (arrows). This cell coat is detached from the cell surface for part of its length. X 30,000

FIG. 77

CEF. Acid phosphatase demonstration by the Gomori method. Dense deposits of lead phosphate end product are associated with a small and a large secondary lysosome (arrows), whilst similar bodies, including a large autolysosome (al), exhibit no deposits. X 52,000

FIG. 78

CEF. Acid phosphatase demonstration by the Gomori method. The deposition of lead phosphate end product indicates that acid phosphatase activity is localised in saccules and vesicles of the Golgi complex (arrows) but not in the autolysosome (al). X 50,000

FIG. 79

ts virus-infected CEF maintained at 35°C. Acid phosphatase demonstration by the Gomori method. Transformed cells such as this contain fewer lysosomes than non-transformed cells. A dense body secondary lysosome (arrow) exhibits lead phosphate end product. Virus particles (v) are found in the extracellular environment. X 26,000

FIG. 80

ts virus-infected CEF maintained at 35°C. Acid phosphatase demonstration by the Gomori method. Enzyme activity is not localised in the vacuoles containing virus particles (v) or, in this particular cell, in the Golgi apparatus. Two small secondary lysosomes (arrows), however, do contain the lead phosphate end product of acid phosphatase activity. X 30,000

FIG. 81

ts virus-infected CEF (35-41-35°C). Acid phosphatase demonstration by the Gomori method. There are more lysosomes than in cells maintained continuously in the transformed state at 35°C. Acid phosphatase activity, as demonstrated by lead phosphate end product deposition, is localised in small secondary lysosomes (small arrows) and in a larger body which is either a late autolysosome or a residual body (large arrow). There is a low level of background lead deposition in nucleus and cytoplasm, unrelated to enzyme activity. Virus particles (v) occur extracellularly and within a vacuole in the cytoplasm. X 15,000

FIG. 82

ts virus-infected CEF (35-41-35^{o}C). Acid phosphatase demonstration by the Gomori method. Amongst extracellular material (ex) are a number of apparently intact secondary lysosomes containing lead phosphate end product. These lysosomes and the accompanying material may have been released from the cell by a process of exocytosis. X 15,000

FIG. 83

ts virus-infected CEF (35-41-35°C). Acid phosphatase demonstration by the Gomori method. A number of virus particles and a secondary lysosome exhibiting lead phosphate end product of acid phosphatase activity appear to have been released from the cell by a process of exocytosis. This may be the means by which lysosomal enzymes are delivered to the cell surface and the extracellular environment. X 52,000

FIG. 84

ts virus-infected CEF (35-41-35°C). Acid phosphatase demonstration by the Gomori method. The middle cell of the three exhibits background lead deposition, unrelated to acid phosphatase activity, throughout its cytoplasm, whereas its two neighbours are completely free of such background deposits. This is a common phenomenon in Gomori preparations. True lead phosphate end product is found in secondary lysosomes (large arrows). It is not clear whether the deposits associated with virus particles (small arrow) are end product or background. X 19,500

FIG. 85

ts virus-infected CEF (35-41-35^{o}C). Acid phosphatase demonstration by the Gomori method. In this well developed Golgi complex acid phosphatase activity, as indicated by lead phosphate end product deposition, is localised within Golgi saccules and vesicles (arrows). Non-enzymic, background lead deposition occurs in the nucleus (N).

X 40,000

FIG. 86

ts virus-infected CEF (35-41^{o}C). Acid phosphatase demonstration by the Gomori method. These cells at the non-permissive temperature for transformation (41^{o}C) are untransformed and adopt the morphology of normal, uninfected CEF cells. Virus particles (v) are still present and the phenomenon of "bubbling" (B) which occurs in the transformed cells (caused by the production and release of masses of vacuoles, see Fig. 120) also persists. Lead phosphate end product of acid phosphatase activity is found in secondary lysosomes (arrows) and amongst extracellular material (ex). X 15,000

FIG. 87

BHK21C13. Cells centrifuged to a pellet prior to incubation for acid phosphatase demonstration by the Gomori method. These cells exhibit lead deposits of varying thickness on the cell surface (arrows). Since similar deposits are encountered in some of the no-substrate controls it is unlikely that they are lead phosphate end product of acid phosphatase activity. Such deposits occur only in cells prepared in this manner. X 15,000

FIG. 88

BHK21C13. Cells centrifuged to a pellet prior to incubation for acid phosphatase demonstration by the Gomori method. Cell surface lead deposits (arrows) are unlikely to indicate acid phosphatase activity since similar deposits can be produced in centrifuged cells incubated in the absence of substrate. Such deposits are occasionally encountered in controls but not in the corresponding test sections.

X 38,500

FIG. 89

3T3. Cells incubated <u>in situ</u> for acid phosphatase demonstration by the Gomori method and then centrifuged to a pellet. This cell has been sectioned in a vertical plane. Dense deposits of lead phosphate end product are found in secondary lysosomes (arrows). X 54,000

FIG. 90

3T3. Cells incubated <u>in situ</u> for acid phosphatase demonstration by the Gomori method and then centrifuged to a pellet. This cell has been sectioned in a vertical plane and the flatter of the two surfaces, that on the right, was probably in contact with the culture dish. Acid phosphatase activity, as indicated by lead phosphate end product deposition, is localised in saccules and vesicles of the Golgi apparatus (small arrows), in dense, homogeneous secondary lysosomes (large arrows) and in an autolysosome (al) where it is associated with a mitochondrion and other material being degraded. Lead deposition which is not a result of enzyme activity occurs in the heterochomatin of the nucleus (N) and to a very small extent in the cytoplasm.

X 39,000

FIG. 91

3T3. Cells incubated <u>in situ</u> for acid phosphatase demonstration by the Gomori method and then centrifuged to a pellet. As in Fig. 90, the flatter surface of this vertically sectioned cell was probably in contact with the culture dish. This surface is covered by a dense layer of lead phosphate end product (small arrows) which may be associated with a cell coat. The other surface exhibits a much sparser end product deposition (large arrow). There are light deposits of non-enzymically derived lead in the nucleus. X 25,000

FIG. 92

SV403T3. Cells incubated <u>in situ</u> for acid phosphatase demonstration by the Gomori method and then centrifuged to a pellet. A large residual body (rb) exhibits some lead phosphate end product deposits, indicating acid phosphatase activity, amongst its content of membranous and amorphous fragments. X 40,000

FIG. 93

BHK21C13, <u>in situ</u> incubated and embedded. LPED procedure for acid phosphatase demonstration. These cells are from a no-substrate control preparation and have exactly the same appearance as those from the test preparations. In both types fine, dense particles of end product-like material occur in certain secondary lysosomes (arrows). The level of deposition is low and many similar lysosomes are totally without deposits. X 48,000

FIG. 94

Mouse kidney cortex. LPED procedure for acid phosphatase demonstration, test preparation. The deposition of fine particles of end product-like material in secondary lysosomes (arrows) is much denser than in BHK21C13 cells (compare Fig. 93). The deposits are of a homogeneous nature. X 75,000

FIG. 95

Mouse kidney cortex. LPED procedure for acid phosphatase demonstration, test preparation. The deposits of end product-like material in the secondary lysosome (arrow) are more irregularly distributed than those of Fig. 94. X 75,000

FIG. 96

Mouse kidney cortex. LPED procedure for acid phosphatase demonstration, test preparation. In the secondary lysosome (arrow) fine particles of dense end product-like material are associated with the membranous structure of a myelin figure. X 52,000

FIG. 97

Mouse kidney cortex. LPED procedure for acid phosphatase demonstration, no-substrate control preparation. Deposition of end product-like material in the secondary lysosome (arrow) is similar to that in the test preparations of Figs. 94 and 95. This indicates that acid phosphatase activity is not required for the production of the deposits.

X 75,000

FIG. 98

Mealworm midgut epithelium. LPED procedure for acid phosphatase demonstration, test preparation. End product-like deposits are confined to a secondary lysosome (arrow) where they are associated with the membranous structure of a myelin figure. X 75,000

FIG. 99

Mealworm midgut epithelium. LPED procedure for acid phosphatase demonstration, no-substrate control preparation. As in the test preparation (Fig. 98) end product-like deposits are associated with the membranous structure of a myelin figure in a secondary lysosome (arrow). X 75,000

FIG. 100

Formol-calcium fixation of BHK21C13 cells followed by incubation for acid phosphatase demonstration by the LPED procedure. The fine structure of this cell is very poorly preserved and no end product or end product-like deposits can be detected. This method of fixation is clearly unsuitable for the electron microscopic investigations being carried out. X 31,500

FIG. 101

Mouse kidney cortex. Lead phthalocyanin procedure for acid phosphatase demonstration, test preparation. The deposition of fine, dense particles of end product-like material in secondary lysosomes (arrows) is very similar to that seen in the LPED preparations (Figs. 94-97). X 75,000

FIG. 102

Mouse kidney cortex. Lead phthalocyanin procedure for acid phosphatase demonstration, test preparation. Deposits of end product-like material are associated with dark, membranous matter in a secondary lysosome (arrow). X 81,000

FIG. 103

Mouse kidney cortex. Lead phthalocyanin procedure for acid phosphatase demonstration, no-substrate control preparation. End product-like deposits occur amongst dark amorphous matter and on membranous material in secondary lysosomes (arrows), just as they do in the test preparations (Figs. 101, 102). X 75,000

FIG. 104

Mouse kidney cortex. Lead phthalocyanin procedure for acid phosphatase demonstration, no substrate control preparation. A myelin figure in a secondary lysosome exhibits fine, dense particles of end product-like material on its component membranes (arrow).

X 78,000

FIG. 105

Mouse kidney cortex incubated in the presence of hexaphenyl lead, a precursor of LPED. There are deposits of fine, particulate, end product-like material (arrows) amongst the dense amorphous contents of a secondary lysosome or residual body. These deposits are similar to those observed in LPED and lead phthalocyanin-treated material.

X 40,000

FIG. 106

Mouse kidney cortex incubated in the presence of triphenyl-p-amino-phenethyl lead, a precursor of LPED. In this very large myelin figure there is a very fine deposition of end product-like material associated with the membranes whilst amongst the amorphous matter in the centre there are coarser deposits. As in Fig. 105, these deposits are similar to those in the LPED and lead phthalocyanin-treated material. X 40,000

FIG. 107

Mouse kidney cortex. The p-nitrobenzene-diazonium tetrafluoroborate (NDFB) procedure for acid phosphatase demonstration, test preparation. End product-like deposits are located in an extracellular myelin figure (arrow), largely associated with membranous material. X 75,000

FIG. 108

Mouse kidney cortex. The p-nitrobenzene-diazonium tetrafluroborate (NDFB) procedure for acid phosphatase demonstration, no-substrate control preparation. As in the test material (Fig. 107) end product-like deposits are associated with the membranous structures of a myelin figure (arrow) within a secondary lysosome. X 75,000

FIG. 109

Mouse kidney cortex. The hexazonium pararosaniline (HPR) procedure for acid phosphatase demonstration, test preparation. A dark, roughly circular profile (arrow), probably part of a secondary lysosome, is associated with deposits of fine, dense particles. As HPR end product is amorphous and simply leads to a slight increase in the density of the organelles with which it is involved, the particulate deposition seen here is unlikely to be end product, although the dark matter with which it is associated might possibly be so. X 60,000

FIG. 110

Mouse kidney cortex. The hexazonium pararosaniline (HPR) procedure for acid phosphatase demonstration, test preparation. Very fine, dense particles are associated with the membranous structure of a myelin figure (arrow) in a secondary lysosome. As in the previous example (Fig. 109) these particles are unlikely to represent HPR end product. No other lysosomes in this field exhibit any evidence of end product.

X 60,000

FIG. 111

Mouse kidney cortex. The hexazonium pararosaniline (HPR) procedure for acid phosphatase demonstration, test preparation. The dense membranous and amorphous material in the secondary lysosome (arrow) is more likely to represent the presence of HPR end product than are the particulate deposits observed in Figs. 109 and 110. X 75,000

FIG. 112

Mouse kidney cortex. The hexazonium pararosaniline (HPR) procedure for acid phosphatase demonstration, no-substrate control preparation. In this field are two large secondary lysosomes or residual bodies containing myelin figures which exhibit a density comparable to that of similar bodies in the test preparations. In addition there is a smaller secondary lysosome (arrow) which is not only very dense but also contains deposits of fine, dense particles. The presence of bodies such as these makes interpretation of HPR results very difficult.

X 40,000

FIG. 113

Mouse kidney cortex. The hexazonium pararosaniline (HPR) procedure for acid phosphatase demonstration, no-substrate control preparations. A number of secondary lysosomes and residual bodies (arrows) contain very dense membranous and amorphous material similar to that observed in test preparations. The density of these components could result from the deposition of electron opaque end product-like material or could be due to their natural osmiophilia. Whichever is the case, they prevent reliable interpretation of results. X 40,000

FIG. 114

Mouse kidney cortex, not subjected to cytochemical tests. Examination of this material reveals that the lysosome population of mouse kidney cortex exhibits a wide range of densities. Some lysosomes, such as the one illustrated (arrow), are not only dense but also contain dense particulate matter which may possibly be confused with end product of a cytochemical reaction. X 78,000

FIG. 115

BHK21J1. Esterase demonstration by the thiolacetic acid method. Spontaneous precipitate formation during incubation has resulted in the appearance within the cells of large dense particles (large arrow). Esterase activity, as indicated by the presence of the fine particulate end product (small arrow), is localised in ER cisternae (er), the matrix of mitochondria (m) and secondary lysosomes (sl). In other sections the enzyme is also localised in saccules and vesicles of the Golgi apparatus. X 40,000

FIG. 116

CEF. Arylsulphatase demonstration by the barium-nitrocatechol sulphate method. This area of cytoplasm contains a great quantity of lysosomes and other vacuoles. Many, but by no means all, of the secondary lysosomes exhibit dense granular deposits of barium sulphate end product of arylsulphatase activity. Within the lysosome the end product is usually concentrated into a discrete, rounded zone occupying up to a third of the organelle (arrows). In certain cases some of the end product has been lost, perhaps during sectioning, leaving a clear space adjacent to or in the centre of the remaining end product.

X 10,000

FIG. 117

CEF. Arylsulphatase demonstration by the barium-nitrocatechol sulphate method. Deposits of barium sulphate end product are concentrated into discrete granular aggregates in homogeneous secondary lysosomes (arrow). This field also provides a good example of the expanded cisternae of rough ER (rer) which are a characteristic feature of normal CEF cells. X 28,000

FIG. 118

CEF. Arylsulphatase demonstration by the barium-nitrocatechol sulphate method. In addition to barium sulphate end product deposition in secondary lysosomes there are also distinct deposits on the inner surface of large vacuole-like bodies with an opaque matrix (arrows).

X 10,800

FIG. 119

ts virus-infected CEF maintained at 35°C. Arylsulphatase demonstration by the barium-nitrocatechol sulphate method. In this transformed cell arylsulphatase activity, as indicated by barium sulphate end product deposition, is localised at three sites. In homogeneous secondary lysosomes the end product is concentrated into dense rounded masses occupying up to a third of the organelle (arrowhead) whilst in a signet ring lysosome it is confined between the two membranes (large arrow). Deposits also occur on the inner surface of a large, apparently empty vacuole (small arrow). X 15,000

FIG. 120

ts virus-infected CEF maintained at 35°C. Arylsulphatase demonstration by the barium-nitrocatechol sulphate method. In this transformed cell barium sulphate end product is aggregated into a dense granular mass, part of which has been lost, in a homogeneous secondary lysosome (large arrow). It is difficult to ascertain whether the very dense material in residual bodies (small arrows) is end product or not. The density of the myelin figures is probably a result of their great osmiophilia. The Golgi complex (G) exhibits no enzyme activity. This cell also displays an example of the "bubbling" phenomenon (B) caused by the release of masses of vacuoles from the cytoplasm. X 20,000

FIG. 121

ts virus-infected CEF maintained at 35°C. Arylsulphatase demonstration by the barium-nitrocatechol sulphate method. Virus particles (v) are contained within a vacuole, presumably a secondary lysosome, which also exhibits arylsulphatase activity, indicated by the granular deposits of barium sulphate end product. Some of the homogeneous secondary lysosomes also contain end product. X 40,000

FIG. 122

ts virus-infected CEF maintained at 35°C. Arylsulphatase demonstration by the barium-nitrocatechol sulphate method. This transformed cell has two very large empty vacuoles which exhibit barium sulphate end product deposits on their inner surface (arrows). End product is also found in homogeneous secondary lysosomes but the Golgi complex (G) is devoid of arylsulphatase activity. X 15,000

FIG. 123

ts virus-infected CEF maintained at 41°C. Arylsulphatase demonstration by the barium-nitrocatechol sulphate method. In this general field deposits of barium sulphate end product, concentrated into rounded masses, can be seen in some of the secondary lysosomes. Unlike the infected cells maintained at 35°C these cells are in the normal state and exhibit many of the characteristic features of the uninfected cells, such as larger lysosome and mitochondrial populations and expanded ER cisternae. End product is more abundant than in the transformed cells but is not as plentiful as that of the uninfected cells.

X 7,800

FIG. 124

ts virus-infected CEF maintained at 41°C. Arylsulphatase demonstration by the barium-nitrocatechol sulphate method. Most of the secondary lysosomes in this cell contain myelin figures and partially digested material in addition to their homogeneous content. Only a few of them exhibit deposits of barium sulphate end product (arrow). X 20,000

FIG. 125

ts virus-infected CEF maintained at 41°C. Arylsulphatase demonstration by the barium-nitrocatechol sulphate method. The presence of numerous small vesicles within most of these secondary lysosomes means that they can probably be classified as multivesicular bodies (mvb). Some also contain endogenous cytoplasmic material in varying stages of breakdown and at least one (arrow) exhibits barium sulphate end product of arylsulphatase activity. There also appear to be two classes of mitochondria, one with a dark matrix (dm) and the other with a light matrix (lm). X 25,000

FIG. 126

ts virus-infected CEF maintained at 41°C. Arylsulphatase demonstration by the barium-nitrocatechol sulphate method. In these cells there are fewer lysosomes than are usually encountered in non-transformed CEF cells and only a small number exhibit barium sulphate end product deposition (arrow). In most other respects the cells are typical of the non-transformed type. X 10,700

FIG. 127

SV403T3. Arylsulphatase demonstration by the barium-nitrocatechol sulphate method. In both normal and transformed 3T3 cells arylsulphatase activity is localised in secondary lysosomes, just as in the chick cells, but in addition barium sulphate end product appears to be located at three further sites. In the transformed cell shown here a lipid droplet (ld) has deposits on the inner surface of its limiting membrane whilst in the Golgi complex (G) there is dense material, possibly end product, in certain of the saccules (small arrow). At the cell surface where there is a narrow intercellular space between two cells there are discrete dense deposits (large arrows) which could also be end product. X 52,000